5750 *Inorg. Chem.* **1994**, *33,* 5750−5753

Methylation of $[PPN][HFe_3(CO)_9SO_2]$

Gail B. Karet, D. M. Norton, Charlotte L. Stern, and Duward F. Shriver*

Department of Chemistry, Northwestern University, Evanston, Illinois 60208-3113

Received February 23, 1994[⊗]

The cluster $[PPN][HFe_3(CO)_9SO_2]$ reacts with $CH_3OSO_3CF_3$ to give $[HFe_3(CO)_9SO_2CH_3]$, which was characterized by infrared and NMR spectroscopy and X-ray crystallography. The methyl group binds to the *exo* oxygen of the coordinated SO_2 ligand in $[PPN][HFe_3(CO)_9SO_2]$. Extended Hückel calculations reveal that SO_2-CH_3 interactions occur through an SO_2 orbital that is not involved in bonding to the metals. Crystallographic data: space group $P\bar{1}$, $a = 8.622(3)$ Å, $b = 14.046(3)$ Å, $c = 15.289(3)$ Å, $\alpha = 69.11(2)°$, $\beta = 77.18(2)°$, $\gamma = 74.74(2)°$.

Introduction

The reactions of SO_2 bound to clusters are of interest from the standpoint of metal cluster assistance of ligand reactivity and also because of potential relationships with the chemistry of SO_2 on metal surfaces.[1] Except for the reduction of coordinated SO_2 in $[PPN][HFe_3(CO)_9SO_2]$, the reduction chemistry of coordinated SO_2 in clusters is an uncharted area.[2−5] In our previous work on electrophile assisted reduction of $[PPN][HFe_3(CO)_9SO_2]$, the attack of acetyl chloride at the exo oxygen of coordinated SO_2 appears to give a weakened S−O bond (eq 1).[5] Upon reduction, this labilization promotes the reductive cleavage of both S−O bonds. The presumed acetylated SO_2 cluster in the above study was too unstable to be isolated,[5] and the present research was undertaken to prepare and structurally characterize a potentially more stable alkylated SO_2 cluster compound.

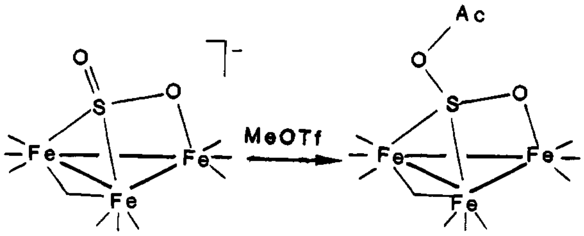

(1)

Experimental Section

Caution! $MeSO_3CF_3$ is highly toxic.

General Information. All manipulations were carried out with standard Schlenk techniques under an atmosphere of prepurified N_2 or on a high-vacuum line.[6] Solids were handled in the oxygen-free N_2 atmosphere of a drybox. Solvents were distilled from appropriate drying agents before use.[7] Solution infrared spectra were recorded on a Bomem MB-Series FTIR spectrometer at 2 cm^{-1} resolution with 0.1 mm path length CaF_2 solution cells, and solids were sampled as Nujol mulls. The ^1H and ^{13}C NMR spectra of ^{13}C-labeled compounds were recorded on a Varian XL-400 spectrometer at 400 and 100 MHz, respectively. The CD_2Cl_2 was vacuum distilled from P_4O_{10} before use, and it served as an internal NMR reference. The $CH_3SO_3CF_3$ was distilled before use. The cluster compound $[PPN][HFe_3(CO)_9SO_2]$ (I) was synthesized by a literature procedure.[5]

Synthesis of $[HFe_3(CO)_9SO_2CH_3]$ (II). A 100 mL Schlenk flask was charged with 330 mg of $[PPN][HFe_3(CO)_9SO_2]$. CH_2Cl_2, 20 mL, was added, followed by 85 μL of $CH_3OSO_2CF_3$. The solution was allowed to stir for 5½ h, during which time it turned from orange-red to red. The product was extracted with 40 mL pentane. Slow removal of the solvent in vacuo, with stirring, yielded red microcrystals of $[HFe_3(CO)_9SO_2CH_3]$. Yield: 30 mg, 19%. IR (pentane; ν_{CO}, cm^{-1}): 2093 (w), 2056 (s), 2041 (vs), 2025 (s), 2015 (w), 2004 (w). IR (Nujol; ν_{SO}, cm^{-1}): 1031, 951.

In a small-scale reaction, a 5 mm NMR tube was charged with 80 mg of $[PPN][HFe_3(CO)_9SO_2]$ and fitted with a septum. CD_2Cl_2 and 30 μL of $CH_3OSO_2CF_3$ was added. ^1H and ^{13}C spectra were acquired at various temperatures on the resulting solution. ^1H NMR (20 °C δ, ppm from TMS): −17.79, 3.83, 4.235, 7.489, 7.668. ^{13}C NMR (20 °C; δ, ppm): 200.5 (br, 2), 209.0 (br, 3), 210.5 (br, 6), 59.99. ^{13}C NMR −90 °C; CO's; δ, ppm): 211.48 (1), 210.29 (2), 209.86 (2), 207.95 (2), 199.28 (2).

Crystal Structure of $[HFe_3(CO)_9SO_2CH_3]$ (II). Crystals were grown from a saturated solution of $[HFe_3(CO)_9SO_2CH_3]$ in pentane kept at −10 °C for a period of 4 days. A red, translucent crystal was mounted using oil (Paratone-n, Exxon) on a glass fiber and placed in the cold stream of an Enraf Nonius CAD4 diffractometer. Unit cell constants were determined by least-squares refinement of the setting angles of 25 unique reflections. A decay correction was not applied, because the intensities of the three reference peaks showed negligible variation. A summary of the data collection is given in Table 1. Lorenz−polarization and analytical absorption corrections were applied with transmission between 0.59 and 0.97.

Calculations were performed with the Texsan 5.0 crystallographic software package. The structure was solved by direct methods (Shelxs-86), with full-matrix least squares refinement. All non-hydrogen atoms were refined with anisotropic thermal parameters. Hydrogen atoms were refined with a group isotropic thermal parameter. The maximum peak in the final difference map was 0.40 e/Å^3, and the minimum peak was −0.42 e/Å^3.

[⊗] Abstract published in *Advance ACS Abstracts,* November 1, 1994.

(1) (a) Siriwardane, R. V.; Cook, J. M. *J. Colloid Interface Sci.* **1985**, *104*, 251. (b) Siriwardane, R. V.; Cook, J. M. *J. Colloid Interface Sci.* **1987**, *116*, 463. (c) Furuyama, M.; Kishi, K.; Ikeda, S. *J. Electron Spectrosc. Relat. Phenom.* **1978**, *13*, 59. (d) Pecora, L. M.; Ficalora, P. J. *Metall. Trans. A* **1977**, *8*, 1841. (e) Wilke, T. D.; Gao, X.; Takaidis, C. G.; Weaver, M. J. *J. Catal.* **1991**, *130*, 62. (f) Bonzel, H. P.; Ku, R. *J. Chem. Phys.* **1973**, *59*, 1641. (g) Kohler, U.; Wassmuth, H. W. *Surf. Sci.* **1982**, *117*, 668. (h) Ku, R. C.; Wynblatt, P. *Appl. Surf. Sci.* **1981**, *8*, 250. (i) Trundle, C. R.; Culey, A. F. *Faraday Discuss. Chem. Soc.* **1975**, *60*, 51.

(2) Ryan, R. R.; Kubas, G. J.; Moody, D. C.; Eller, P. C. *Struct. Bonding (Berlin)* **1981**, *46*, 47.

(3) Mingos, D. M. P. *Transition Met. Chem. (Weinheim)* **1978**, *3*, 1.

(4) W. A. Schenk, *Angew. Chem., Int. Ed. Engl.* **1987**, *26*, 98.

(5) Karet, G. B.; Stern, C. L.; Norton, D. M.; Shriver, D. F. *J. Am. Chem. Soc.* **1993**, *115*, 9979.

(6) Shriver, D. F.; Drezdzon, M. A. *The Manipulation of Air-Sensitive Compounds*, 2nd ed.; Wiley: New York, 1986.

(7) Gordon, A. J.; Ford, R. A. *The Chemist's Companion*; Wiley: New York, 1972.

0020-1669/94/1333-5750$04.50/0

Table 1. X-ray Crystallographic Structure Data for [$HFe_3(CO)_9SO_2CH_3$]

formula: $Fe_3SO_{11}C_{10}H_4$	fw: 499.74
$a = 8.622(3)$ Å	space group: $P\bar{1}$ (No. 2)
$b = 14.046(3)$	$t = -120$ °C
$c = 15.289(3)$ Å	$\lambda = 0.710\ 69$ Å
$\alpha = 69.11(2)°$	$\varrho_{calcd} = 2.009$ g cm^{-3}
$\beta = 77.18(2)°$	$\mu = 27.74$ cm^{-1}
$\gamma = 74.74(2)°$	$R(F_o) = 0.031^a$
$Z = 4$	$R_w(F_o) = 0.034^b$

^{a} $R = \sum(|F_o| - |F_c|)/\sum|F_o|$. ^{b} $R_w = [\sum w(|F_o| - |F_c|)^2/\sum w|F_o|^2]^{1/2}$; w $= \sigma_{F_o}{}^{-2}$.

Calculational Details. Extended Hückel calculations were performed with CACAO.[8,9] Calculations were performed utilizing idealized symmetry. Similar overlap populations and energy levels were obtained with the crystallographic coordinates of the cluster for [PPN][$Fe_3(CO)_9SO_2$]. Axial carbonyl ligands were taken to be perpendicular to the plane of an equilateral metal triangle, and equatorial carbonyls were placed in the plane of the triangle, 116° apart. For [$HFe_3(CO)_9SO_2$]$^-$ and [$HFe_3(CO)_9SO_2CH_3$], the O−S, O−M, and O−C distances used were those found for these clusters by X-ray diffraction. The Fe−O−S and O−S−O angles were chosen to approximate those found by X-ray crystallography. Atomic parameters are the same as those used previously.[10]

Results and Discussion

Methylation of [PPN][$HFe_3(CO)_9SO_2$] (I). [PPN][$HFe_3(CO)_9SO_2$] (**I**) reacts with $MeSO_3CF_3$ to give the neutral cluster [$HFe_3(CO)_9SO_2CH_3$] (**II**), eq 2.

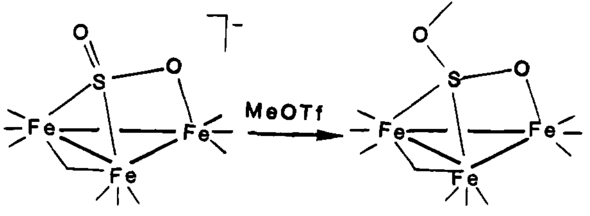

(2)

A crystal structure of [$HFe_3(CO)_9SO_2CH_3$] (**II**) demonstrates that an oxygen-bound sulfinate complex has formed. The unit cell contains two crystallographically unique but essentially similar clusters. An ORTEP drawing of one of the clusters is shown in Figure 1. The [CH_3]$^+$ group, as expected from mull infrared data, binds to the *exo* oxygen of the coordinated SO_2 ligand. The O−C distances for the methylated oxygen of SO_2 (Table 2), 1.44(1), 1.444(9) Å, for the two crystallographically independent [$HFe_3(CO)_9SO_2CH_3$] molecules, are shorter than the O−C distance in [SO_2CH_3][AsF_6] (1.502(9) Å).[11]

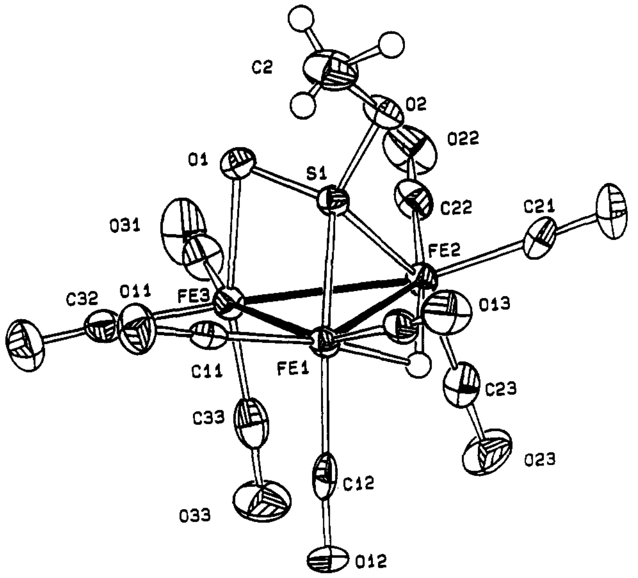

Figure 1. ORTEP drawing of one of the clusters in the unit cell of [$HFe_3(CO)_9SO_2CH_3$]. Thermal ellipsoids are drawn at the 50% probability level.

Table 2. Selected Interatomic Distances for [$HFe_3(CO)_9SO_2CH_3$]

Fe1−Fe2	2.675(2)	Fe1−Fe3	2.629(2)
Fe2−Fe3	2.656(1)	Fe4−Fe5	2.680(2)
Fe5−Fe6	2.638(2)	Fe4−Fe6	2.640(2)
Fe1−S1	2.096(2)	Fe2−S1	2.086(2)
Fe3--S1	2.408(2)	Fe4−S2	2.077(2)
Fe5−S2	2.101(2)	Fe6--S2	2.420(2)
Fe3−O1	2.078(4)	Fe6−O3	2.070(4)
Fe1−H1	1.60(7)	Fe2−H1	1.71(8)
Fe4−H2	1.64(8)	Fe5−H2	1.65(7)
S1−O1	1.511(5)	S1−O2	1.603(4)
S2−O3	1.512(4)	S2−O4	1.602(4)
O2−C2	1.44(1)	O4−C4	1.444(9)
C2−H2A	0.84(9)	C2−H2B	1.14(8)
C2−H2C	0.70(9)	C4−H4A	1.09(8)
C4−H4B	0.96(9)	C4−H4C	0.74(9)

Bond distances and angles for [$HFe_3(CO)_9SO_2CH_3$] also show that attack of the $CH_3OSO_2CF_3$ distorts the SO_2 ligand. The distance between the sulfur and the *exo* oxygen of SO_2 lengthens from 1.434(9) Å in [PPN][$HFe_3(CO)_9SO_2$][5] to 1.602(4) or 1.603(4) Å in [$HFe_3(CO)_9SO_2CH_3$]. The metal-bound S−O bond is shortened from 1.62 Å in **I** to 1.511(5) or 1.512(4) Å in [$HFe_3(CO)_9SO_2CH_3$] (**II**).[5] A mull infrared spectrum reveals that the two S−O stretching frequencies (1031, 951 cm^{-1}) have shifted upon methylation. In keeping with the changes in bond length, the high frequency S−O stretch is over 100 cm^{-1} lower in **II** than in **I** and the low frequency stretch shifts to higher wavenumbers.[5] Both the X-ray and vibrational data suggest that the attack of Me$^+$ weakens the bond between sulfur and the *exo* oxygen of SO_2 but that the converse is true for the metal-bound oxygen.

The bonded Fe−S and Fe−O distances in [$HFe_3(CO)_9SO_2CH_3$] (Fe−S 2.077(2)−2.101(2) Å, Fe−O 2.070(4) and 2.078(4) Å) are similar to those in [PPN][$HFe_3(CO)_9SO_2$],[5] and the nonbonded Fe3−S distance in **I** (2.602(5) Å) decreases to 2.408(2) and 2.420(2) Å in **II**.

The hydride ligand was directly located by X-ray crystallography, and its position was confirmed by NMR spectroscopy. The ^1H and ^{13}C NMR spectra indicate that the structure of the cluster in solution correlates with that in the solid state. The ^1H resonance at −17.79 ppm suggests that the hydride ligand bridges two iron atoms. A ^1H resonance at 3.83 ppm and a ^{13}C resonance at 59.99 ppm are assigned to the protons and carbon, respectively, of the O-bound methyl group.

At −90 °C the carbonyl region of the $^{13}C\{^1H\}$ NMR spectrum of **II** has five resonances at 211.32 (1 CO), 210.15 (2 CO's), 209.77 (2 CO's), 207.71 (2 CO's), and 199.14 (2 CO's) ppm. The resonances at 211.32 and 207.71 ppm broaden at 0 °C and then coalesce into a single broad peak at 209 ppm at 20 °C. They are assigned to the carbonyl ligands on the iron bound to the oxygen. Those at 210.15 and 209.77 ppm coalesce into a single peak 210.2 ppm by −60 °C. At room temperature the

---

[8] (a) Hoffmann, R.; Lipscomb, W. N. *J. Chem. Phys.* **1962**, *36*, 2179. (b) Hoffman, R.; Lipscomb, W. N. *J. Chem. Phys.* **1962**, *36*, 3489. (c) Hoffmann, R.; Lipscomb, W. N. *J. Chem. Phys.* **1962**, *37*, 2872. (d) Hoffmann, R. *J. Chem. Phys.* **1963**, *39*, 1397.

[9] Mealli, C.; Proserpio, D. M. *J. Chem. Educ.* **1990**, *67*, 399.

[10] (a) Daniels, J. M.; Dorain, P. B. *J. Chem. Phys.* **1966**, *45*, 26. (b) Carrington, A.; Levy, D. H. *J. Phys. Chem.* **1967**, *71*, 2.

[11] Minkwitz, R.; Bernstein, D.; Preut, H.; Sawodny, W.; Härtner, H. *Z. Anorg. Allg. Chem.*, **1991**, *606*, 157.

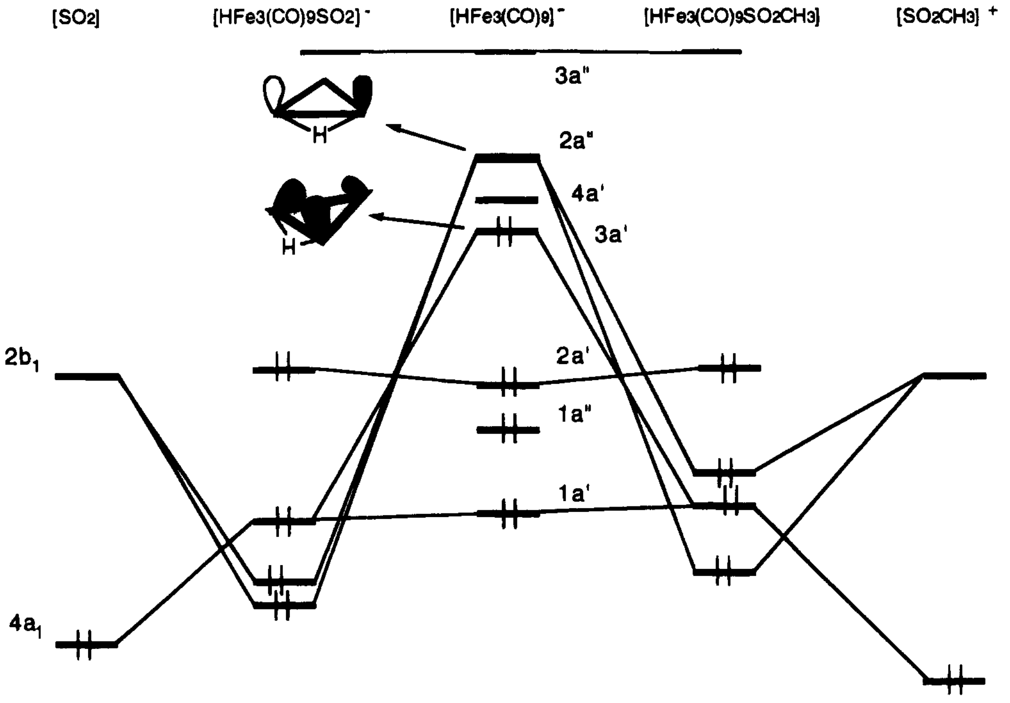

Figure 2. Energy level diagram showing the interaction of $[HFe_3(CO)_9]^-$ with SO_2 and $[SO_2CH_3]^+$.

resonances at 210.2 and 200.5 ppm appear to be broadened by slow intrametallic exchange of the carbonyls on the other two iron atoms. A plane of symmetry lies through the sulfur and oxygens of the sulfur dioxide ligand. The only location for a bridging hydride that maintains this plane of symmetry is between the two iron atoms bridged by the sulfur. In the absence of ^1H decoupling, the resonance at 209.77 ppm at −90 °C is split, $J_{C-H} = 9$ Hz, which is consistent with the crystal structure and the ^{13}C NMR assignments.

The crystal structure of **II** confirms the spectroscopic evidence for alkylation of the *exo* oxygen of SO_2. Precedence for this mode of interaction is found in the structure of $[Ru(CO)_2(\eta^2\text{-}SO_2{\cdot}SO_2)(PPh_3)_2]$, for which a second SO_2 molecule acts as a Lewis acid, binding through sulfur to the *exo* oxygen of the coordinated SO_2.[12] The distance between the *exo* oxygen and the second SO_2 is over 2.5 Å, because the interaction with SO_2 is much weaker than that with $[CH_3]^+$ in $[HFe_3(CO)_9SO_2CH_3]$. Another related example is the dimerization of $[Mo(CO)_2(PPh_3)(py)(\eta^2\text{-}SO_2)]$ to form $[Mo(CO)_2(PPh_3)(py)(\eta^2\text{-}SO_2)]_2$ in which each Mo coordinates to the *exo* oxygen of an $\eta^2\text{-}SO_2$ ligand on the other molybdenum atom.[2,13]

Molecular Orbital Calculations. Calculations were performed to explore the changes in bonding between the capping ligand and $[HFe_3(CO)_9]^-$ that occur upon electrophilic attack of SO_2. By analogy to the changes observed with the formation of C- and O-bonded CO, increases in $M{-}SO_2$ π back-bonding were expected upon alkylation of the exo oxygen.[14] We chose to describe the interactions in terms of an $[HFe_3(CO)_9]^-$ fragment combining with either SO_2 or $[SO_2CH_3]^+$. Although this description provides a physically appealing distribution of electrons in the parent fragments, in the Hückel approximation, it does not influence the orbital energies.

The frontier orbitals of $[Fe_3(CO)_9]^{2-}$ have been previously discussed in detail.[15] An added H^+ interacts with two of the iron atoms of $[Fe_3(CO)_9]^{2-}$ through one component of the 1e orbitals, which lie in the Fe_3 plane. Because $[HFe_3(CO)_9]^-$ has C_s symmetry, the e orbitals of $[Fe_3(CO)_9]^{2-}$ split into a′ and a″ orbitals (Figure 2). In the 3a′ orbital, as in the $2a_1$ orbital from which it is derived, a lobe on each iron points toward the capping ligand. The lobes for the 2a″ orbital also are positioned to overlap significantly with the sulfur atom of the capping ligand. The 1a′, 1a″, and 2a′ orbitals, like the 1e and $1a_1$ orbitals of $[Fe_3(CO)_9]^{2-}$, do not project toward the capping SO_2.

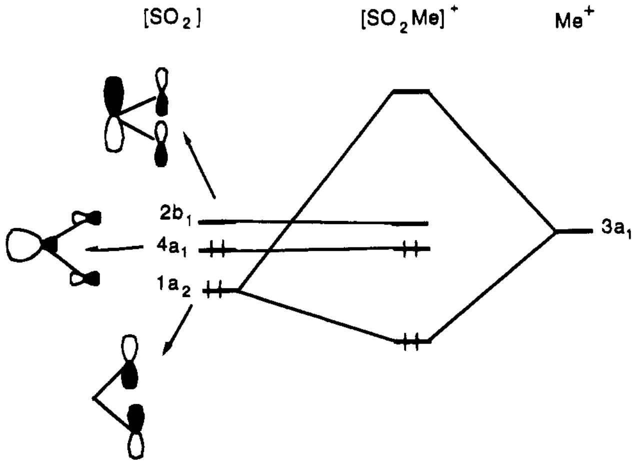

Figure 3. Energy level diagram showing the interaction of free $[SO_2]^{2-}$ with CH_3^+.

The electronic structure of free SO_2 has been extensively studied.[2] When the CH_3^+ is placed perpendicular to the plane of the SO_2, the $1a_2$ orbital, made up of oxygen p_x orbitals, interacts with the LUMO of $[CH_3]^+$, Figure 3. Of greatest importance in binding to single metals are the $4a_1$ and $2b_1$ orbitals of SO_2.[3] Both of these orbitals lie mainly on sulfur but have some oxygen p character.[3] Both are uninvolved in binding to $[CH_3]^+$ and are the only contributors to the HOMO and LUMO of $[SO_2CH_3]^+$.

---

(12) Jarvinen, G. D.; Kubas, G. J.; Ryan, R. R. *J. Chem. Soc., Chem. Commun.* **1981**, 305.

(13) Moody, D. C.; Ryan, R. R. *J. Chem. Soc., Chem. Commun.*, **1980**, 1230.

(14) Horwitz, C. P.; Shriver, D. F. *Adv. Organomet. Chem.* **1984**, *23*, 219.

(15) Schilling, B. E. R.; Hoffmann, R. *J. Am. Chem. Soc.* **1979**, *101*, 3456.

The interactions of SO_2 and $[SO_2Me]^+$ with the metal triangle are similar, Figure 2. The HOMO's of SO_2 and $[SO_2CH_3]^+$ participate in σ bonding with the 3a′ orbital of $[HFe_3(CO)_9]^-$. Metal−ligand π bonding occurs between the $[HFe_3(CO)_9]^-$ 2a″ orbital and the LUMO's of SO_2 and $[SO_2CH_3]^+$.

Reduced overlap populations between iron and sulfur in [$HFe_3(CO)_9SO_2CH_3$] suggest that the sulfur interacts only weakly with the iron bound to an oxygen of $[SO_2CH_3]^+$. The reduced overlap population between this iron and the sulfur (21) is roughly $^1/_{30}$th of the reduced overlap population between the other two irons and sulfur (608).

Weakening of the C−O bond upon attack of an electrophile on the oxygen of a bridging carbonyl ligand by an electrophile has been attributed to increased π back-bonding between the carbonyl and the metals.[14] By contrast, bonding between CH_3^+ and SO_2 gives rise to an orbital which is located mainly on the oxygens and which is uninvolved in metal−ligand π bonding. The orbital responsible for M−L π bonding is largely unaffected by attachment of CH_3^+. Consequently, the calculated charges on the iron atoms and the carbonyl ligands change only slightly from $[HFe_3(CO)_9SO_2]^-$ to [$HFe_3(CO)_9SO_2CH_3$]. Changes in calculated charge occur mainly for the oxygen to which CH_3^+ binds (−1.3 in $[HFe_3(CO)_9SO_2]^-$, −0.8 in [$HFe_3(CO)_9SO_2CH_3$]).

As with the MO calculations, the vibrational data indicate little increase in π back-bonding from iron to sulfur dioxide upon O-alkylation of the coordinated μ_3,η^2-SO_2 ligand. Specifically, the average ν_{CO} shifts from 2017 cm^{-1} in **I** to 2041 cm^{-1} in **II**, but this 24 cm^{-1} shift is smaller than the observed shift (58 cm^{-1}) for the strong terminal carbonyl stretching frequencies when $[HFe_3(CO)_{11}]^-$ is alkylated to produce $HFe_3(CO)_{10}(COCH_3)$.[16]

Acknowledgment. This work was supported by DOE through Grant DE-FG02-86ER13640.

Supplementary Material Available: Listings of all positional parameters, anisotropic thermal parameters, complete bond distances and angles, torsion or conformation angles, and crystallographic data (13 pages). Ordering information is given on any current masthead page.

---

[16] Hodali, H. A.; Shriver, D. F. *Inorg. Chem.* **1979**, *18*, 1236.